Radiology

Comparison of Symptomatic and Asymptomatic Atherosclerotic Carotid Plaque Features with in Vivo MR Imaging[1]

Tobias Saam, MD
Jianming Cai, MD, PhD
Lin Ma, MD, PhD
You-Quan Cai, MD
Marina S. Ferguson, MT
Nayak L. Polissar, PhD
Thomas S. Hatsukami, MD
Chun Yuan, PhD

Purpose: To retrospectively determine if in vivo magnetic resonance (MR) imaging can simultaneously depict differences between symptomatic and asymptomatic carotid atherosclerotic plaque.

Materials and Methods: Institutional review board approval and informed consent were obtained for this HIPAA-compliant study. Twenty-three patients (21 men, two women; mean age, 66.1 years $\pm$ 11.0 [standard deviation]) with unilateral symptomatic carotid disease underwent 1.5-T time-of-flight MR angiography and 1.5-T T1-, intermediate-, and T2-weighted MR imaging. Both carotid arteries were reviewed. One observer recorded quantitative and morphologic information, which included measurement of the area of the lumen, artery wall, and main plaque components; fibrous cap status (thick, thin, or ruptured); American Heart Association (AHA) lesion type (types I–VIII); and location (juxtaluminal vs intraplaque) and type of hemorrhage. Plaques associated with neurologic symptoms and asymptomatic plaques were compared with Wilcoxon signed rank and McNemar tests.

Results: Compared with asymptomatic plaques, symptomatic plaques had a higher incidence of fibrous cap rupture ($P = .007$), juxtaluminal hemorrhage or thrombus ($P = .039$), type I hemorrhage ($P = .021$), and complicated AHA type VI lesions ($P = .004$) and a lower incidence of uncomplicated AHA type IV and V lesions ($P = .005$). Symptomatic plaques also had larger hemorrhage ($P = .003$) and loose matrix ($P = .014$) areas and a smaller lumen area ($P = .008$). No significant differences between symptomatic and asymptomatic plaques were found for quantitative measurements of the lipid-rich necrotic core, calcification, and the vessel wall or for the occurrence of intraplaque hemorrhage or type II hemorrhage.

Conclusion: This study revealed significant differences between symptomatic and asymptomatic plaques in the same patient.

© RSNA, 2006

Radiology

Atherosclerosis is a systemic disease of the vessel wall, and the majority of established risk factors for atherosclerosis are systemic in nature (1). Although plaques tend to develop at focal sites, it appears that a link exists between atherosclerotic disease in various sites of the vascular tree. For example, studies have shown that peripheral vascular disease and carotid artery atherosclerosis may indicate the presence of coronary artery disease (2). Adams et al (3) found that atherosclerotic lesions develop symmetrically in the left and right carotid arteries. Our experience has shown that with rare exceptions patients with symptomatic carotid artery atherosclerosis have substantial contralateral carotid disease. However, given that symptomatic and asymptomatic carotid lesions develop in the same genetic and environmental milieu, why do the neurologic complications of atherosclerosis have a propensity to develop unilaterally?

Much of what is currently known about differences between symptomatic and asymptomatic carotid plaques is based on histologic analysis of excised carotid endarterectomy specimens (4). Atherosclerosis research based on histologic analysis, however, is constrained by three factors inherent in its design. First, a histologic examination is invasive; thus, information pertaining to plaque can be obtained at only one time point. Second, during carotid endarterectomy, the tube-like carotid plaque is cut length wise and it is frequently torn, thus preventing accurate gross or microscopic assessment (5). Third, histologic findings from the asymptomatic plaque of the contralateral artery are unavailable; therefore, symptomatic plaques are typically compared with

asymptomatic plaques from a different group of patients, thus making it difficult to control for all genetic and environmental atherosclerotic risk factors.

Studying features of asymptomatic and symptomatic plaques in the same patient at the same time is an ideal way to control for all known and unknown risk factors of atherosclerosis. This approach would eliminate the environmental, genetic, and temporal variability inherent in histologic comparisons of lesions in symptomatic patients with those in asymptomatic patients.

Studies have shown that magnetic resonance (MR) imaging can be used to accurately characterize and quantify the composition and morphology of human carotid atherosclerotic plaque in vitro and in vivo, including the lipid-rich necrotic core, calcification, fibrous cap status, age and location of hemorrhage or thrombus, and American Heart Association (AHA) lesion type (6–13). The purpose of this study was to retrospectively determine if in vivo MR imaging can simultaneously depict differences between symptomatic and asymptomatic carotid atherosclerotic plaque.

Materials and Methods

Our study was compliant with the Health Insurance Portability and Accountability Act, and it was approved by the institutional review board of each institution that contributed patient studies. Consent forms signed by patients at the time of imaging allowed retrospective analysis of patient studies and data.

Patients

Between April 1998 and February 2003, bilateral carotid arteries of 27 consecutive patients with neurologic symptoms were examined with MR imaging after patients provided informed consent. Patients were included if (a) they had a history of transient ischemic attack, amaurosis fugax, or stroke appropriate to the distribution of the index carotid artery; (b) they had not previously undergone carotid endarterectomy; (c) the time between onset of symptoms and MR imaging was 4 months or less; (d) carotid stenosis, as measured with duplex

ultrasonography on the symptomatic side, was at least 50%; and (e) bilateral identical coverage of MR imaging (ie, distance covered by MR imaging in the craniocaudal direction) was at least 1.2 cm. Four patients with an image quality score of less than 3, as scored with a five-point scale (1 = poor, 5 = excellent [10]), were excluded.

The remaining 23 patients (21 men, two women; mean age, 66.1 years ± 11.0 [standard deviation] [Table 1]) underwent a complete neurologic examination performed by a vascular surgeon with more than 10 years of clinical experience (T.S.H.). When clinically indicated, neurologic consultation was provided by faculty members in the department of neurology (University of Washington, Seattle, Wash) and additional diagnostic tests—including brain computed tomography, MR imaging, echocardiography, and Holter monitoring—were used to rule out other potential causes of symptoms. The median interval between symptom onset and MR imaging was 1.5 months, the standard deviation was 1.3 months, and the range was 1 week to 4 months.

MR Imaging Protocol

Imaging was performed with a 1.5-T MR imager (Signa Horizon EchoSpeed; GE Healthcare, Waukesha, Wis) and a phased-array surface coil (Pathway MRI, Seattle, Wash) (14). This coil included two modules for the bilateral ca-

Advances in Knowledge

- MR imaging features differ between symptomatic and asymptomatic plaques.
- Preliminary evidence shows that hemorrhage location (intraplaque hemorrhage vs juxtaluminal hemorrhage or thrombus) and type may influence symptoms.

rotid arteries, and it was combined with a head holder that comfortably prevented neck rotation; thus, subjects remained in a stable position. A standardized protocol (15) was used to obtain four transverse images of the carotid arteries with four different imaging parameters.

T1-, intermediate-, and T2-weighted MR imaging and three-dimensional time-of-flight (TOF) angiography were performed. Parameters for black-blood double inversion-recovery two-dimensional fast spin-echo T1-weighted MR imaging were as follows: repetition time msec/echo time msec, 800.0/9.3–11.0; echo train length, eight; acquisition time, 8 minutes; and 12 sections acquired. Parameters for double-echo fast spin-echo cardiac-gated intermediate- and T2-weighted MR imaging were as follows: 2500–3700/10–20 (effective) for intermediate-weighted imaging; 2500–3700/40–70 (effective) for T2-weighted imaging; three or four R-R intervals; echo train length, eight; acquisition time, 3–4 minutes; and 18 sections acquired. Parameters for three-dimensional TOF angiography were as follows: 23.0/3.5; flip angle, 25°; acquisition time, 3 minutes; and 40 sections acquired.

All examinations were performed with a 13–16-cm field of view, a matrix of 256 × 256 pixels, a 2-mm section thickness, and two acquired signals. An intersection space of −1 mm was used for three-dimensional TOF angiography, whereas no intersection space was used for MR imaging. Imaging examinations were centered on the bifurcation. Fat suppression was used for T1-, intermediate-, and T2-weighted MR imaging to reduce the signal from subcutaneous fat. Zero-filled Fourier transformation was used to reduce pixel size, which ranged from 0.25 × 0.25 mm to 0.31 × 0.31 mm, depending on the field of view, and to minimize partial-volume artifacts.

Image Review

Both carotid arteries were reviewed. One radiologist (T.S., with more than 2 years of experience in the interpretation of carotid plaque images) rated the quality of each image before the review

by using a previously published five-point scale; scores were dependent on the overall signal-to-noise ratio (13). A score of 1 indicated the arterial wall and vessel margins were unidentifiable. A score of 2 indicated the signal-to-noise ratio was marginal, the arterial wall was visible, and the substructure, lumen, and outer boundaries were indistinct. A score of 3 indicated the wall structures were identifiable but the lumen and outer boundaries were partially obscured. A score of 4 indicated the signal-to-noise ratio was high and the vessel wall and lumen margins were well defined. A score of 5 indicated the signal-to-noise ratio was excellent and the vessel wall and lumen margins could be

detected in every detail. For each imaging location, four images obtained with different parameters were available for review. Only the locations of the carotid arteries ipsilateral to symptoms that had corresponding matching locations in the contralateral carotid artery, with regard to longitudinal distance from the bifurcation point, were analyzed. The continuous mean coverage was 1.7 cm for both arteries. All MR images were examined by the same radiologist, who was blinded to patients' clinical information at the time of image analysis.

Plaque composition and quantitative measurements.—Areas of the lumen, outer wall, and plaque tissue components were measured with a quantita-

Table 1

Baseline Clinical Data

Characteristic and Risk Factor	Finding
Age (y)*	66.1 ± 11.0 (45–81)
Male sex	91 (21/23)
Height (m)*	1.72 ± 0.08 (1.55–1.85)
Weight (kg)*	76.8 ± 13.7 (59–98)
Body mass index (kg/m^2)*	25.6 ± 3.7 (20.3–34.8)
Hypertension	83 (18/22)
Diabetes	4 (1/23)
History of smoking	59 (13/22)
History of coronary artery disease	39 (9/23)
Hypercholesterolemia	74 (17/23)
Use of lipid-lowering medication	33 (7/23)

Note.—Unless otherwise indicated, data are percentages and data in parentheses were used to calculate percentages.

* Data are mean ± standard deviation. Numbers in parentheses are the range.

Table 2

Plaque Composition and Plaque Burden

Tissue Type	Symptomatic Arteries (mm^2)	Asymptomatic Arteries (mm^2)	P Value*
Lumen area	26.6 ± 14.0	35.1 ± 13.9	.008
Wall area	47.8 ± 17.0	44.0 ± 20.4	.3
Outer wall area	74.4 ± 26.9	79.1 ± 31.4	.3
Lipid-rich necrotic core	8.1 ± 6.3	6.3 ± 5.7	.2
Hemorrhage area	3.5 ± 3.4	1.1 ± 1.5	.003
Calcification area	3.1 ± 6.6	2.7 ± 6.1	.2
Loose matrix area	2.3 ± 2.7	0.9 ± 1.1	.014

Note.—Unless otherwise indicated, data are the mean area per location in an artery ± standard deviation.

* P values were calculated with the Wilcoxon signed rank test.

tive vascular image analysis system, which is a custom-designed image analysis tool (16). The area circumscribed by the outer wall boundary included the lumen, intima, media, and adventitia. The wall area was calculated by subtracting the lumen area from the outer wall area. Plaque tissue components, such as the lipid-rich necrotic core, hemorrhage, calcification, and loose matrix, were identified by using previously published MR imaging criteria (7,10,13). All signal intensities were compared with the sternocleidomastoid muscle at a point adjacent to and at the same depth as the carotid arteries.

Plaque morphology.—Lesion type was determined at each location according to a previously published modified AHA classification scheme (6).

The fibrous cap was categorized as intact and thick (type I), intact and thin (type II), or ruptured (type III) (8). Intact and thick fibrous caps had a uniform continuous dark band adjacent to the lumen on TOF angiograms and a smooth lumen surface on TOF angiograms and T1-, intermediate-, and T2-weighted MR images. Intact and thin fibrous caps had no visible dark band adjacent to the lumen on TOF angiograms and a smooth lumen surface on TOF angiograms and T1-, intermediate-, and T2-weighted MR images. Ruptured fibrous caps had a disrupted dark band or no visible dark band adjacent to the lumen on TOF angiograms; an irregular lumen boundary on TOF angiograms and T1-, intermediate-, and T2-weighted MR images; and a hyperintense area adjacent to the lumen on TOF angiograms. The highest possible rating was assigned to each artery, and plaques were categorized as intact and thick, intact and thin, or ruptured.

Two patients were excluded from fibrous cap analysis: One had a calcified lesion without a fibrous cap, and one had a TOF angiogram with an image quality score of less than 3. Juxtaluminal calcification appeared as a hypointense area on images obtained with all four parameters. It was not discernable from the lumen on black-blood images, but it was clearly distinguishable from the bright lumen on TOF angiograms.

Hemorrhage was differentiated by location (juxtaluminal vs intraplaque) and type (type I vs type II). A hemorrhage or thrombus was considered juxtaluminal if the region of interest was adjacent to the lumen and the dark juxtaluminal band was absent on TOF angiograms (9). Intraplaque hemorrhage was defined as a hemorrhage located deep within the plaque or near the luminal surface, with MR imaging evidence of an intact thick cap (9). Criteria for determining the hemorrhage type were based on previously published MR imaging criteria, with a modification in the terminology. The terms *type I* and *type II* rather than *fresh* and *recent,* respectively, were used to describe the age of intraplaque hemorrhage (7). Type I hemorrhage was histologically characterized by intact red blood cells with intracellular methemoglobin. A type I hemorrhage appeared hyperintense on TOF angiograms and T1-weighted im-

Table 3

AHA Lesion Type Distribution

AHA Lesion Type	Description	Symptomatic Arteries (%)	Asymptomatic Arteries (%)	P Value*
I	Normal wall	4.3 ± 10.6	8.2 ± 18.4	.2
III	Eccentric plaque, no calcification	6.5 ± 10.8	4.5 ± 8.5	.5
Combined IV and V	Lesion with lipid-rich necrotic core	15.6 ± 16.7	34.5 ± 30.7	.005
VI	Complicated lesion	63.3 ± 25.2	40.7 ± 31.5	.004
VII	Calcified lesion	5.6 ± 10.7	7.6 ± 17.2	.5
VIII	Lesion with fibrosis	0.0 ± 0.0	0.7 ± 3.4	.3

Note.—Unless otherwise indicated, data are mean ± standard deviation.

* P values were calculated with the Wilcoxon signed rank test.

Table 4

Luminal Surface Status and Hemorrhage by Type and Location

Characteristic	Symptomatic Plaques	Asymptomatic Plaques	P Value*
Fibrous cap status			
Thick	0 (0)	5 (22)	.06
Thin	3 (13)	9 (39)	.1
Ruptured	18 (78)	7 (30)	.007
Other (no fibrous cap or image quality < 3 on TOF images)	2 (9)	2 (9)	>.999
Hemorrhage of any type present at any location	23 (100)	20 (87)	.3
Hemorrhage type			
I (fresh)	20 (87)	12 (52)	.021
II (recent)	22 (96)	18 (78)	.2
Hemorrhage location			
Intraplaque	21 (91)	19 (83)	.5
Juxtaluminal or thrombus	14 (61)	6 (26)	.039
Luminal calcification and adjacent hemorrhage	13 (57)	9 (39)	.2

Note.—Unless otherwise indicated, data are number of patients. Data in parentheses are percentages.

* P values were calculated with the McNemar test.

ages and iso- to hypointense on inter-mediate- and T2-weighted images. A type II hemorrhage was histologically characterized by lytic red blood cells with extracellular methemoglobin and ap-peared hyperintense on all images (7).

Statistical Analysis

All locations that could be matched with the contralateral artery were used for statistical analysis. Each patient con-tributed only one set of observations (one study of the symptomatic arteries, one study of the asymptomatic arteries) to the data set for analysis. Area mea-surements for each artery were calcu-lated as the mean area measured per location for each artery separately. For AHA lesion types, the percentage of sections showing a specific lesion type was calculated for each artery. The mean AHA lesion type distributions cal-culated for symptomatic arteries were compared with those calculated for asymptomatic arteries. For all other categorical variables, the percentage of arteries that showed the selected fea-ture at one or more locations was calcu-lated separately for symptomatic and asymptomatic arteries. To better ac-commodate the abnormal distribution of some of the variables, nonparametric tests were used to compare the symp-tomatic and asymptomatic arteries. The Wilcoxon signed rank test was used to compare variables that were areas or the proportion of sections with a speci-fied AHA lesion type. The McNemar test was used to compare all categorical variables. Because of the limited sample size, the significance of the difference in proportions with the McNemar test was calculated with binomial distribution, as described by Lehman (17). Computation was performed with SPSS for Windows, versions 12 and 13 (SPSS, Chicago, Ill). Differences were considered significant if the P value was less than .05.

Results

Image Quality

Mean image quality was similar be-tween symptomatic and asymptomatic arteries (3.8 vs 3.7, $P = .5$).

Figure 1
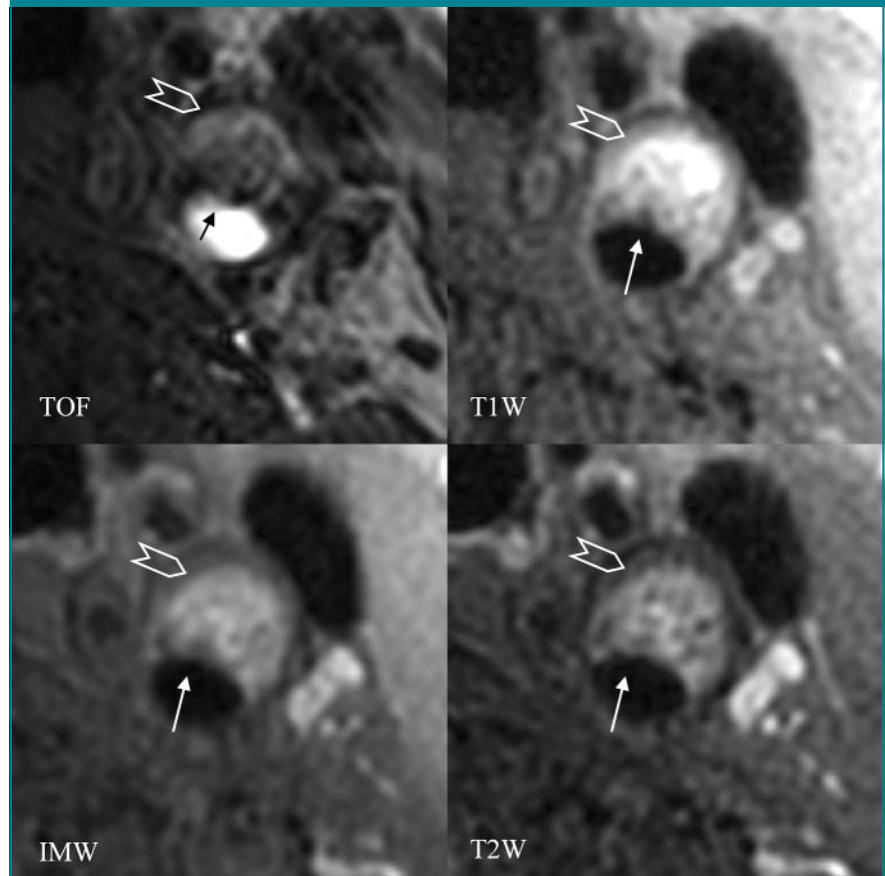
Figure 1: Transverse MR images of a complicated AHA type VI lesion in the left common carotid artery of an 81-year-old patient who experienced ipsilateral neurologic symptoms 3 months before MR imaging. A surface irregularity and a hyperintense juxtaluminal signal (arrow) visible on the TOF angiogram (23.0/3.5) indicate a fibrous cap rupture or ulcer. A hyperintense area (chevron) visible on TOF, T1-weighted *(T1W)* (800.0/9.3), intermediate-weighted *(IMW)* (3500/10), and T2-weighted *(T2W)* (3500/40) images indicates a necrotic core with type II hemorrhage.

Lumen and Wall Area

The degree of atherosclerotic burden in symptomatic arteries was similar to that in asymptomatic arteries in terms of mean wall area (47.8 mm^2 vs 44.0 mm^2, $P = .3$) and mean outer wall area (74.4 mm^2 vs 79.1 mm^2, $P = .3$) (Table 2). In contrast, symptomatic arteries had a significantly smaller mean lumen area than did asymptomatic arteries (26.6 mm^2 vs 35.1 mm^2, $P = .008$).

Plaque Composition

No significant differences between symp-tomatic and asymptomatic arteries were found for calcification areas ($P = .2$) or lipid-rich necrotic core areas ($P = .2$)

(Table 2). Symptomatic arteries had a larger hemorrhage area (3.5 mm^2 vs 1.1 mm^2, $P = .003$) and a larger loose matrix area (2.3 mm^2 vs 0.9 mm^2, $P = .014$) than did asymptomatic arteries.

Lesion Type

In our study, 95.7% of the symptomatic arteries exhibited atherosclerotic le-sions classified as AHA type III or greater, whereas 91.8% of the asymp-tomatic arteries exhibited similar ath-erosclerotic lesions. Complicated type VI lesions (plaques with a luminal sur-face defect, hemorrhage, or thrombus) (Figs 1, 2) were found more frequently in symptomatic arteries than in asymp-

tomatic arteries (63.3% vs 40.7%, P = .004) (Table 3). In contrast, uncomplicated type IV and V lesions (plaques with lipid-rich or necrotic cores and surrounding fibrous tissue) (Fig 3) were found more frequently in asymptomatic arteries than in symptomatic arteries (34.5% vs 15.6%, P = .005). No significant differences were found among the other lesion types.

Fibrous Cap

Plaques associated with neurologic symptoms were categorized as ruptured more often than were contralateral asymptomatic plaques (78% vs 30%, P = .007) (Table 4). Conversely, symptomatic plaques were categorized as intact and thick (0% vs 22%, P = .06) or intact and thin (13% vs 39%, P = .1) less often than were asymptomatic plaques; however, these differences were not significant. One artery on each side was excluded from fibrous cap analysis because the image quality score of TOF angiograms was less than 3. One patient was excluded because the heavily calcified lesion in both carotid arteries did not have a fibrous cap.

Location and Type of Hemorrhage

Intraplaque hemorrhage was a common finding in both symptomatic and asymptomatic plaques. Specifically, 91% of patients with symptomatic plaques and 83% of patients with asymptomatic plaques had at least one location of intraplaque hemorrhage (P = .5) (Table 4). However, juxtaluminal hemorrhage or thrombus was 2.3 times more common in patients with symptomatic plaques than in patients with asymptomatic plaques (61% vs 26%, P = .039).

Type II (recent) hemorrhage was common in patients with symptomatic plaques and in those with asymptomatic plaques; 96% of patients with symptomatic plaques and 78% of patients with asymptomatic plaques had at least one location of type II hemorrhage (P = .2) (Table 4). Type I (fresh) hemorrhage occurred 1.7 times more often in patients with symptomatic plaques than in those with asymptomatic plaques (87% vs 52%, P = .021).

Luminal Calcification

Juxtaluminal calcification with adjacent hemorrhage was slightly more common in patients with symptomatic plaques than in patients with asymptomatic plaques (57% vs 39%); however, this difference was not significant (P = .2) (Table 4).

Discussion

High-spatial-resolution imaging allowed us to obtain quantitative and morphologic information in both the symptomatic and the asymptomatic arteries simultaneously and noninvasively, thereby providing an internal control for the external environment and for genetic and temporal variations.

Our findings show that substantial plaque burden was noted in both carotid arteries, as indicated by the mean wall area (47.8 mm^2 vs 44.0 mm^2, P = .3) and the mean outer wall boundary area (74.4 mm^2 vs 79.1 mm^2, P = .3) for the symptomatic and asymptomatic sides, respectively. Both carotid arteries exhibited advanced plaque features, such as necrotic core, hemorrhage, loose fibrous matrix, and calcification. Furthermore, the number of locations with AHA type III through type VIII lesions in the symptomatic arteries was comparable with that in the asymptomatic arteries (96% vs 92%).

Plaque composition (measured in
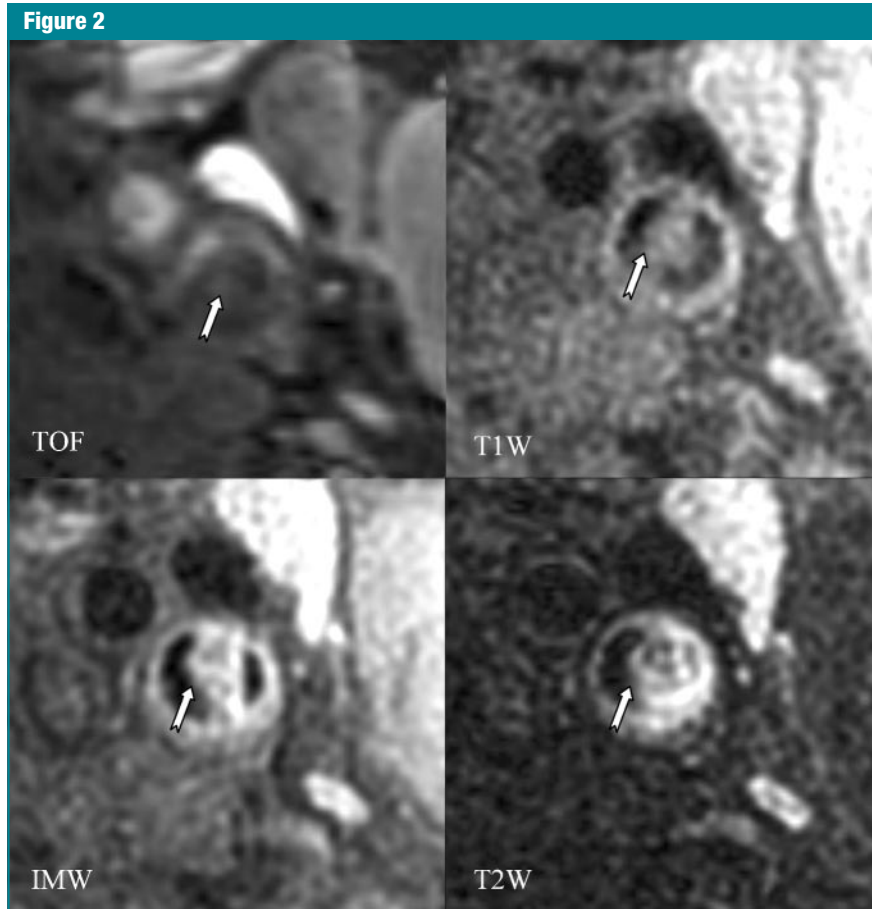
Figure 2

Figure 2: Transverse TOF (23.0/3.5) MR angiogram and T1-weighted *(T1W)* (800.0/9.3), intermediate-weighted *(IMW)* (2769/10), and T2-weighted *(T2W)* (2769/70) MR images of a complicated AHA type VI lesion in the left internal carotid artery of a 48-year-old patient who experienced four episodes of amaurosis fugax in the 4 months before MR imaging. An irregularly shaped intraluminal hyperintense area (arrow) is visible on intermediate- and T2-weighted images in the left internal carotid artery. This finding is indicative of mural thrombus.

square millimeters) was comparable on both sides for lipid-rich necrotic core and calcification. This finding was supported by histologic findings in the carotid arteries, where symptomatic and asymptomatic plaques showed no differences in the size of the lipid-rich necrotic core (18,19) or the amount of calcification (8,18).

Loose matrix and hemorrhage areas were larger in symptomatic arteries than in asymptomatic arteries. Previous work has shown that a loose matrix is produced in plaque healing (ie, repair of a fibrous cap rupture that involves loose matrix) of coronary arteries in patients with silent plaque rupture (20) and that the larger amount of loose matrix formation in the symptomatic artery may occur in response to previous fibrous cap ruptures in this artery.

The association of hemorrhage and symptoms remains a controversial subject (21–24). Lusby et al (23) suggested that intraplaque hemorrhage and surface thrombosis were cardinal features of symptomatic plaques. Sitzer et al (25) demonstrated that ulceration and luminal thrombosis were the main sources of downstream cerebral microemboli in patients with high-grade internal carotid artery stenosis. Kolodgie et al (26) found evidence that showed a hemorrhage might represent a potent atherogenic stimulus. Other studies (4,19,27) found no hemorrhagic differences between symptomatic and asymptomatic plaques, although these studies did not consider the hemorrhage location (intraplaque vs juxtaluminal) or type (I vs II).

In our study, when hemorrhage prevalence was considered independently from hemorrhage location or type, no significant difference was found between symptomatic and asymptomatic plaques. However, when hemorrhages were categorized as type I (fresh) or type II (recent), type I hemorrhages were found significantly more often in patients with symptomatic plaques than in patients with asymptomatic plaques (87% vs 52%, respectively; *P* = .021). Conversely, the prevalence of type II hemorrhage was comparable in patients with symptomatic

Figure 3
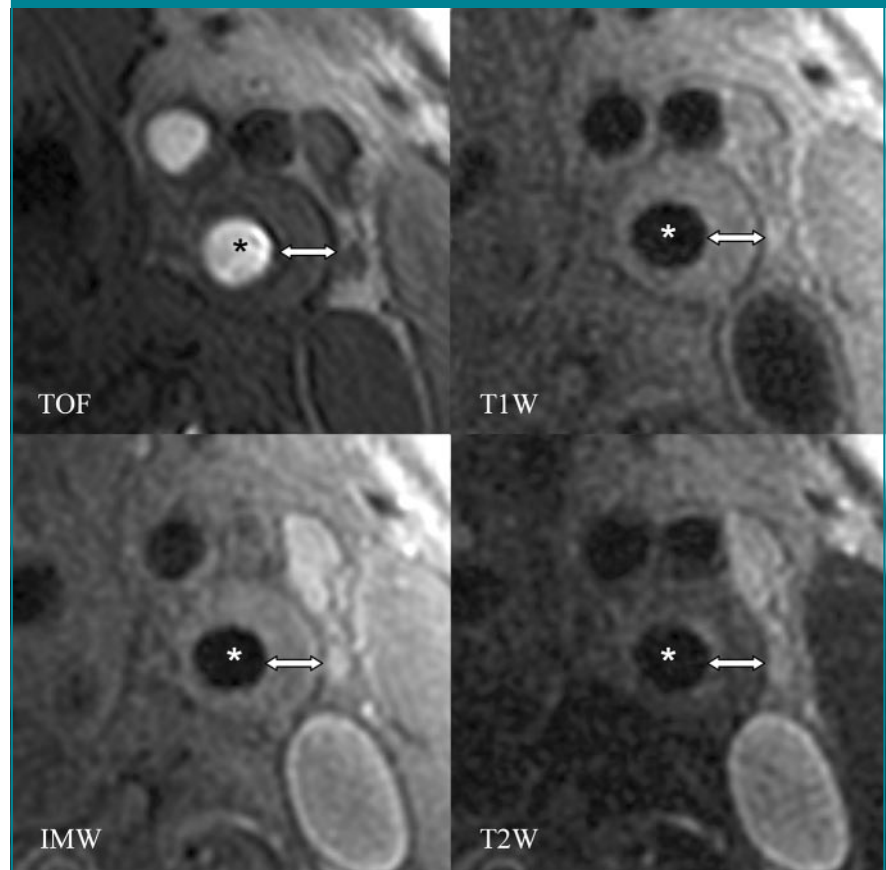
Figure 3: Transverse TOF (23.0/3.5) MR angiogram and T1-weighted *(T1W)* (800.0/9.3), intermediate-weighted *(IMW)* (3000/10), and T2-weighted *(T2W)* (3000/70) MR images of an uncomplicated type IV and V lesion in the left internal carotid artery (∗) on the asymptomatic side in a 62-year-old patient. The homogeneous appearance of the eccentric plaque (arrow) on T1-, intermediate-, and T2-weighted MR images, with a smooth lumen surface and a dark band on TOF MR angiograms, indicates the presence of a thick fibrous cap.

plaques and those with asymptomatic plaques. The higher prevalence of type I hemorrhage in patients with symptomatic plaques is characterized by intact red blood cells at histologic analysis and could be caused by either repeated intraplaque hemorrhages or influx of red blood cells from the luminal surface due to a surface defect, such as fibrous cap rupture. We used the terms type I and type II rather than fresh and recent on the basis of an evolving understanding of the distinct time course of intraplaque hemorrhage in the carotid artery. Findings of a recent MR imaging study (28) indicate that atherosclerotic intraplaque hemorrhages may have a longer course for change than that of

intracranial hemorrhages because of inherent differences in the tissue environment within the lipid-rich necrotic core. When hemorrhages were categorized according to their location as either an intraplaque hemorrhage or a juxtaluminal hemorrhage or thrombus, the prevalence of intraplaque hemorrhage was comparable between symptomatic and asymptomatic plaques; however, a juxtaluminal hemorrhage or thrombus was found significantly more often in patients with symptomatic plaque than in patients with asymptomatic plaque (61% vs 26%, respectively; *P* = .039). These findings indicate that the hemorrhage location in relation to the surface and the hemorrhage type

and age are important when determining a patient's symptom status.

Symptomatic plaques had significantly more fibrous cap ruptures than did asymptomatic plaques (78% vs 30%, respectively; $P = .007$). Other authors (29–32) noted that a ruptured or thin fibrous cap is an important feature of vulnerable coronary artery plaque. Our findings indicate that fibrous cap status is also a critical characteristic of high-risk carotid artery lesions. Furthermore, our findings are in agreement with those of Yuan et al (33), who showed that a significant correlation exists between a patient's in vivo fibrous cap status and symptom status.

Complications associated with juxtaluminal plaque structures and luminal surface conditions were reflected by differences in AHA lesion types observed in symptomatic and asymptomatic arteries. Symptomatic arteries had significantly more complicated type VI lesions with possible surface defects, thrombus, and hemorrhage than did asymptomatic arteries (63% vs 41%, $P = .004$). In contrast, type IV and V lesions were more common in asymptomatic arteries and reflected the absence of complications, such as fibrous cap rupture, hemorrhage, and thrombus.

Our results show that the proximity of the necrotic core to the lumen (expressed as thickness of the fibrous cap), the proximity of hemorrhage to the luminal surface, and the prevalence of type I hemorrhage are associated with neurologic symptoms. Other plaque features, such as the quantitative measurements of lipid-rich necrotic cores and calcifications, or indicators of plaque burden, such as outer wall and wall areas, showed no correlation with neurologic symptoms. These results support the findings of Bassiouny et al (18), who examined a carotid endarterectomy specimen and showed that the topography of individual plaque components in relation to the luminal surface can be used to determine the symptomatic outcome.

A limitation of our study was that the median time between symptom onset and MR imaging was 1.5 months. Lesion characteristics may change during that time. The time between symptom onset and MR imaging should be decreased in future studies.

Although we found highly significant differences between symptomatic and asymptomatic plaques, the predictive value of these findings must be determined in a longitudinal study.

Although both symptomatic and asymptomatic arteries showed features of advanced atherosclerotic disease, the asymptomatic arteries showed less luminal narrowing. It has yet to be determined which of the significant differences in the characteristics of symptomatic and asymptomatic carotid atherosclerotic lesions observed in our study are due to increased luminal narrowing and which produce symptoms.

Only MR images of at least average quality were considered for review; thus, four patients were excluded from analysis. Furthermore, one artery on each side was excluded from fibrous cap analysis because the image quality score of TOF angiograms was less than 3. Improvements in MR imaging protocols, such as time-efficient multisection double inversion-recovery imaging (34) and contrast material–enhanced quadruple inversion-recovery imaging (35), have improved the exclusion rate (36). The exclusion rate should continue to improve in conjunction with improvements in pulse sequence design and hardware (higher-field-strength MR imaging and improved coil design).

In conclusion, the noninvasive imaging approach used in our study revealed significant differences in the composition and morphology of both symptomatic and asymptomatic plaques in the same patient. High-spatial-resolution in vivo MR imaging might be used to characterize high-risk plaque and ultimately identify at-risk patients.

References

1. Fuster V, Fayad ZA, Badimon JJ. Acute coronary syndromes: biology. Lancet 1999; 353(suppl 2):SII5–SII9.

2. Lekakis JP, Papamichael CM, Cimponeriu AT, et al. Atherosclerotic changes of extra-coronary arteries are associated with the extent of coronary atherosclerosis. Am J Cardiol 2000;85:949–952.

3. Adams GJ, Simoni DM, Bordelon CB Jr, et al. Bilateral symmetry of human carotid artery atherosclerosis. Stroke 2002;33:2575–2580.

4. Golledge J, Greenhalgh RM, Davies AH. The symptomatic carotid plaque. Stroke 2000; 31:774–781.

5. Fisher M, Paganini-Hill A, Martin A, et al. Carotid plaque pathology: thrombosis, ulceration, and stroke pathogenesis. Stroke 2005; 36:253–257.

6. Cai JM, Hatsukami TS, Ferguson MS, Small R, Polissar NL, Yuan C. Classification of human carotid atherosclerotic lesions with in vivo multicontrast magnetic resonance imaging. Circulation 2002;106:1368–1373.

7. Chu B, Kampschulte A, Ferguson MS, et al. Hemorrhage in the atherosclerotic carotid plaque: a high-resolution MRI study. Stroke 2004;35:1079–1084.

8. Hatsukami TS, Ross R, Polissar NL, Yuan C. Visualization of fibrous cap thickness and rupture in human atherosclerotic carotid plaque in vivo with high-resolution magnetic resonance imaging. Circulation 2000;102: 959–964.

9. Kampschulte A, Ferguson MS, Kerwin WS, et al. Differentiation of intraplaque versus juxtaluminal hemorrhage/thrombus in advanced human carotid atherosclerotic lesions by in vivo magnetic resonance imaging. Circulation 2004;110:3239–3244.

10. Saam T, Ferguson MS, Yarnykh VL, et al. Quantitative evaluation of carotid plaque composition by in vivo MRI. Arterioscler Thromb Vasc Biol 2005;25:234–239.

11. Serfaty JM, Chaabane L, Tabib A, Chevallier JM, Briguet A, Douek PC. Atherosclerotic plaques: classification and characterization with T2-weighted high-spatial-resolution MR imaging—an in vitro study. Radiology 2001; 219:403–410.

12. Toussaint JF, LaMuraglia GM, Southern JF, Fuster V, Kantor HL. Magnetic resonance images lipid, fibrous, calcified, hemorrhagic, and thrombotic components of human atherosclerosis in vivo. Circulation 1996;94: 932–938.

13. Yuan C, Mitsumori LM, Ferguson MS, et al. In vivo accuracy of multispectral magnetic resonance imaging for identifying lipid-rich necrotic cores and intraplaque hemorrhage in advanced human carotid plaques. Circulation 2001;104:2051–2056.

14. Hayes CE, Mathis CM, Yuan C. Surface coil phased arrays for high-resolution imaging of

the carotid arteries. J Magn Reson Imaging 1996;6:109–112.

15. Yuan C, Mitsumori LM, Beach KW, Maravilla KR. Carotid atherosclerotic plaque: noninvasive MR characterization and identification of vulnerable lesions. Radiology 2001;221:285–299.

16. Kerwin WS, Han C, Chu B, et al. A quantitative vascular analysis system for evaluation of atherosclerotic lesions by MRI. In: Niessen WJ, Viergever MA, eds. Medical Image Computing and Computer-Assisted Intervention—MICCAI 2001. Lecture Notes in Computer Science. Vol 2208. Berlin, Germany: Springer, 2001; 786–794.

17. Lehman EL. Nonparametrics: statistical methods based on ranks. New York, NY: Holden-Day, 1975; 268–269.

18. Bassiouny HS, Sakaguchi Y, Mikucki SA, et al. Juxtalumenal location of plaque necrosis and neoformation in symptomatic carotid stenosis. J Vasc Surg 1997;26:585–594.

19. Hatsukami TS, Ferguson MS, Beach KW, et al. Carotid plaque morphology and clinical events. Stroke 1997;28:95–100.

20. Burke AP, Kolodgie FD, Farb A, et al. Healed plaque ruptures and sudden coronary death: evidence that subclinical rupture has a role in plaque progression. Circulation 2001;103:934–940.

21. Davies MJ. Stability and instability: two faces of coronary atherosclerosis—the Paul Dudley White lecture 1995. Circulation 1996;94:2013–2020.

22. Fryer JA, Myers PC, Appleberg M. Carotid intraplaque hemorrhage: the significance of neovascularity. J Vasc Surg 1987;6:341–349.

23. Lusby RJ, Ferrell LD, Ehrenfeld WK, Stoney RJ, Wylie EJ. Carotid plaque hemorrhage: its role in production of cerebral ischemia. Arch Surg 1982;117:1479–1488.

24. Moody AR, Murphy RE, Morgan PS, et al. Characterization of complicated carotid plaque with magnetic resonance direct thrombus imaging in patients with cerebral ischemia. Circulation 2003;107:3047–3052.

25. Sitzer M, Muller W, Siebler M, et al. Plaque ulceration and lumen thrombus are the main sources of cerebral microemboli in high-grade internal carotid artery stenosis. Stroke 1995;26:1231–1233.

26. Kolodgie FD, Gold HK, Burke AP, et al. Intraplaque hemorrhage and progression of coronary atheroma. N Engl J Med 2003;349:2316–2325.

27. Carr S, Farb A, Pearce WH, Virmani R, Yao JS. Atherosclerotic plaque rupture in symptomatic carotid artery stenosis. J Vasc Surg 1996;23:755–765.

28. Takaya N, Yuan C, Chu B, et al. Presence of intraplaque hemorrhage stimulates progression of carotid atherosclerotic plaques: a high-resolution magnetic resonance imaging study. Circulation 2005;111(21):2768–2775.

29. Davies MJ, Thomas AC. Plaque fissuring: the cause of acute myocardial infarction, sudden ischaemic death, and crescendo angina. Br Heart J 1985;53:363–373.

30. Falk E. Coronary thrombosis: pathogenesis and clinical manifestations. Am J Cardiol 1991;68(7):28B–35B.

31. Fuster V, Stein B, Ambrose JA, Badimon L, Badimon JJ, Chesebro JH. Atherosclerotic plaque rupture and thrombosis: evolving concepts. Circulation 1990; 82(3 suppl): II47–II59.

32. Virmani R, Kolodgie FD, Burke AP, Farb A, Schwartz SM. Lessons from sudden coronary death: a comprehensive morphological classification scheme for atherosclerotic lesions. Arterioscler Thromb Vasc Biol 2000; 20:1262–1275.

33. Yuan C, Zhang SX, Polissar NL, et al. Identification of fibrous cap rupture with magnetic resonance imaging is highly associated with recent transient ischemic attack or stroke. Circulation 2002;105:181–185.

34. Yarnykh VL, Yuan C. Multislice double inversion-recovery black-blood imaging with simultaneous slice reinversion. J Magn Reson Imaging 2003;17:478–483.

35. Yarnykh VL, Yuan C. T1-insensitive flow suppression using quadruple inversion-recovery. Magn Reson Med 2002;48:899–905.

36. Saam T, Kerwin WS, Chu B, et al. Sample size calculation for clinical trials using magnetic resonance imaging for the quantitative assessment of carotid atherosclerosis. J Cardiovasc Magn Reson 2005;7(5):799–808.